On the use of acrylated epoxidized soybean oil as a reactive compatibilizer in injection-molded compostable pieces consisting of polylactide filled with orange peel flour

L. Quiles-Carrillo[1], N. Montanes[1], J.M. Lagaron[2], R. Balart[1], S. Torres-Giner[1,2*]

[1] *Technological Institute of Materials (ITM), Universitat Politècnica de València, Plaza Ferrándiz y Carbonell 1, 03801 Alcoy, Spain*

[2] *Novel Materials and Nanotechnology Group, Institute of Agrochemistry and Food Technology (IATA), Spanish Council for Scientific Research (CSIC), Calle Catedrático Agustín Escardino Benlloch 7, 46980 Paterna, Spain*

** Corresponding author: storresginer@iata.csic.es and storresginer@upv.es*

Abstract. In the present study, novel green composites made of polylactide (PLA) and orange peel flour (OPF) were melt compounded by twin-screw extrusion (TSE) and shaped into pieces by injection molding. Orange peel, a large by-product of the juice industry, was first grounded to flour and then incorporated as a lignocellulosic filler into the biopolymer at 10, 20, and 30 wt.-%. Since both components of the green composite presented low compatibility, the resultant injection-molded pieces showed poor ductility and impaired thermomechanical performance. As a new bio-based reactive compatibilizer, acrylated epoxidized soybean oil (AESO) was added at 5 parts per hundred resin (phr) to the PLA/OPF formulations during the extrusion process. The addition of AESO increased the filler–biopolymer adhesion and led to compostable green composite pieces with improved physical properties. The enhancement achieved was related to a dual effect of plasticization and melt grafting of the OPF particles onto the PLA chains provided by the multiple acrylate and epoxy groups present in AESO. The use of multi-functionalized vegetable oils to improve the performance of green composites certainly opens up new opportunities for the expansion of fully bio-based and biodegradable materials that are partially obtained from agro-food waste.

Keywords: *PLA, Green composites, Multi-functionalized vegetable oils, Reactive extrusion, Waste valorization*

1. Introduction

Nowadays, the increasing environmental concern about the extensive use of petroleum-derived polymers is leading the research of new environmentally friendly polymer materials obtained from natural resources.[1] The development of green composites is a leap forward to solve these environmental problems since these novel materials combine a bio-based polymer with a natural filler obtained either from plants or agro-food wastes.[2, 3] Additionally, the use of biodegradable polymers, that is, polymers that undergo rapidly and completely disintegration through the action of enzymes and/or chemical deterioration associated with living microorganisms, represents the most valuable approach in green composites since fully bio-based and biodegradable materials are produced.[4, 5]

The use of polylactide (PLA) as the matrix in green composites is currently gaining a great importance.[6, 7] Indeed, this biopolyester is nowadays considered the front runner in the bioplastics market, which is already surpassing some conventional polymers derived from petroleum with an annual consumption of 140,000 tons.[8] PLA is of particular interest in the manufacturing of green composites due to its dual-fold advantage of being bio-based and biodegradable.[9, 10] In addition, it shows the required mechanical strength for different industrial applications (*e.g.* automotive, rigid packaging or building and construction) as well as adequate thermal stability and rheological characteristics for being easily processable and recyclable at the large scale.[11-13]

The latest research performed on green composites shows that the employ of lignocellulosic materials obtained from industrial by-products and food or agroforestry wastes is increasing as cost-effective fillers since they provide a sustainability

enhancement and improve the physical performance.[14, 15] Some recent examples include, for instance, wood flour,[16] banana fibers,[17] rice husk,[18, 19] peanut skin,[20, 21] wheat and soy fibers,[22] pita fibers,[23] and *Posidonia oceanica* seaweed.[24] In the present study, it is intended to use, for the first time, orange peel flour (OPF) as the lignocellulosic filler to develop green composites of PLA. The use of this lignocellulosic filler provides a further positive sustainable effect on the resultant green composite due to the large world production of oranges and, especially, to the possibility of generating a high added value from a readily available residue produced by the juice industry. Indeed, around 20 million tons of solid and liquid wastes derived from the orange juice production are globally generated. In this sense, Spain is one of the main world producers of oranges, among other countries like Brazil, the United States, and China, being the Valencian Community one of the areas with the highest production rate with approximately 1.7 million tons of oranges.[25] Although at present orange peel is not of economic value, it is rich in cellulose, sugars, hemicellulose, pectin, and essential oils, which opens up new opportunities for diverse applications.[26]

There are some general drawbacks related to the use of lignocellulosic fillers in polymer composites, which are mainly derived from their poor interfacial adhesion with most polymer and biopolymer matrices. In general, polymers are highly hydrophobic whilst the lignocellulosic materials are extremely hydrophilic. This low chemical affinity is certainly responsible for their lack of compatibility, thus leading to the formation of particle aggregates and, in overall, poor physical properties.[17, 27, 28] In this sense, reactive extrusion (REX) has been proposed as a smart strategy to enhance the properties of polymer materials, being particularly interesting for the preparation of biopolymer blends.[29] Based on this concept, REX has been recently proposed as a novel route for grafting inorganic nanoparticles with polar surface onto biopolymer matrices,

which results in polymer nanocomposites with enhanced physical properties.[30] This process is based on the addition during melt mixing of reactive additives capable of acting as interfacial agents between both components of the polymer composite. This process particularly involves the chemical attachment of the fillers to the biopolymer chains by the action of reactive molecules with an average functionality (*f*) value of, at least, 2. These additives cannot only act as interfacial agents but they can also potentially react with hydrolyzed polymer chains to provide a chain-extension effect, inducing a positive effect on melt stability.[31, 32]

Most conventional and commercially available reactive additives consist of polymers with a low molecular weight (M_W) or oligomers based on different functional groups, such as anhydride, epoxy, oxazoline, isocyanates, acrylates, etc.[33, 34] More recently, however, the use of chemically modified vegetable oils (*e.g.* maleinized, acrylated, and epoxidized oils), the so-called multi-functionalized vegetable oils, has been expanded.[35, 36] The multi-functionalized vegetable oils present the dual advantage of being derived from natural resources and of acting as plasticizers due to their intrinsic lubricant effect on polymer matrices.[37] This is of great interest from an environmental point of view since they allow obtaining totally ecofriendly and fully bio-based polymer formulations with improved toughness.[38-40] In this regard, chemically modified oils, such as maleinized linseed oil (MLO)[41] or epoxidized soybean oil (ESO),[42] have been recently used to increase the filler–matrix compatibility in PLA-based composites with very promising results. The main objective of the present work is to evaluate the effect of acrylated epoxidized soybean oil (AESO) on the compatibility and physical properties of injection-molded green composite pieces consisting of PLA and OPF.

2. Experimental

2.1. Materials

A commercial PLA grade Ingeo^{TM} biopolymer 6201D was obtained from NatureWorks (Minnetonka, MN, USA). This PLA resin is characterized by a density of a density of 1.24 g/cm^3 and a melt flow index (MFI) of 15–30 g/10 min (210 °C and 2.16 kg), which makes it suitable for injection molding. Fresh oranges were purchased in a local market in Valencia. AESO was supplied by Sigma-Aldrich S.A. (Madrid, Spain). According to the supplier, this contains 4000 ppm of monomethyl ether hydroquinone as inhibitor to avoid polymerization.

2.2. Preparation of orange peel flour

The orange peels were first allowed to dry for 48 h at 40 °C using a dehumidifying stove MCP Vacuum Casting System (Lubeck, Germany) to remove any residual moisture. Then, the dried peels were crushed in a Maype mill (Manises, Spain) to reduce their particle size for facilitating their incorporation into the centrifugal mill. The resultant particles were further allowed to dry at 40 °C for 12 h. The peel particles were then milled by means of a Mill ZM 200 centrifugal mill from Retsch (Düsseldorf, Germany) at a speed of 12,000 rpm and finally sieved with a 250-μm mesh filter. The different stages carried out during the preparation of OPF are shown in **Figure 1**.

2.3. Preparation of green composite pieces

Prior to processing, all materials were dried at 60 °C for 36 h in a dehumidifying dryer MDEO from Industrial Marsé (Barcelona, Spain) to remove any residual moisture due to the high sensitiveness of PLA to hydrolysis. Materials were then melt compounded in a co-rotating twin-screw extruder from Construcciones Mecanicas Dupra S.L. (Alicante, Spain). The screws feature 25 mm diameter with a length (L) to diameter (D) ratio, that is, L/D, of 24. All materials, namely PLA, OPF, and AESO, were fed using the main hopper. The temperature profile was set as follows: 180 ºC (feeding zone), 185 ºC, 190 ºC, and 195 ºC (die). A rotating speed of 20 rpm was selected. Residence time was

about 1 min, measured by means of a blue masterbatch. The AESO content was fixed at 5 parts per hundred resin (phr) based on recent previous research performed for this multi-functionalized vegetable oil,[43] while the amount of OPF in the PLA formulations varied from 10 to 30 wt.-%. A neat PLA sample and a green composite sample at 10 wt.-% without AESO were produced in the same conditions as the control materials. **Table 1** summarizes the set of the prepared formulations.

The resultant PLA and green composites pellets were shaped into pieces by injection molding. This was carried out in a Sprinter 11 machine from Erinca S.L (Cornellá, Spain). The temperature profile was set as follows: 170 ºC (hopper), 175 ºC, 180 ºC, and 185 ºC (injection nozzle). The materials were injected into a mirror-finishing steel mold with standard geometries for sample characterization. A clamping force of 11 tons was applied. The cavity filling and cooling time were set at 1 and 10 s, respectively. Standard samples with a thickness of 4 mm were obtained. The obtained pieces were stored in a desiccator at 25 ºC and 0% relative humidity (RH) for 1 week.

2.4. Morphology

The morphology of the OPF particles and the fracture surfaces of the green composite pieces after the impact tests were observed by field emission scanning electron microscopy (FESEM) in a ZEISS ULTRA 55 from Oxford Instruments (Abingdon, United Kingdom). The working distance (WD) varied in the 6–7 mm range and an extra high tension (EHT) of 2 kV was applied to the electron beam. Before placing samples in the FESEM vacuum chamber, the surfaces were coated with a gold-palladium alloy in a sputter coater EMITECH model SC7620 from Quorum Technologies, Ltd. (East Sussex, UK). OPF sizes were determined using Image J Launcher v 1.41 and the data presented were based on measurements from a minimum of 50 SEM micrographs.

2.5. Thermal characterization

Main thermal transitions of the green composites were obtained by differential scanning calorimetry (DSC) in a Mettler-Toledo 821 calorimeter (Schwerzenbach, Switzerland). An average sample weight ranging from 5 to 7 mg was subjected to a heating step from 40 ºC to 190 ºC at a heating rate of 10 ºC min^{-1}. All tests were run in nitrogen atmosphere with a flow-rate of 66 mL min^{-1} using standard sealed aluminum crucibles of a volume capacity of 40 µL. The degree of crystallinity (X_C) was determined by the following expression (**Eq. 1**):

$$X_C\ (\%) = \left[\frac{\Delta H_m - \Delta H_{CC}}{\Delta H_m^0 \cdot (1-w)}\right] \cdot 100 \qquad \textbf{Equation 1}$$

Where ΔH_m and ΔH_{CC} (J/g) stand for the normalized melt and cold crystallization enthalpies respectively, ΔH_m^0 (J g^{-1}) represents the melt enthalpy of a theoretically fully crystalline PLA, that is, 93 J g^{-1},[44] and 1-*w* corresponds to the weight fraction of PLA in the formulation.

Thermal stability was determined by thermogravimetric analysis (TGA) in a Mettler-Toledo TGA/SDTA 851 thermobalance (Schwerzenbach, Switzerland). Samples with an average weight of 5–7 mg were placed in standard alumina crucibles of 70 µL and subjected to a heating program from 30 ºC to 700 ºC at a heating rate of 20 ºC min^{-1} in air atmosphere.

2.6. Mechanical characterization

Tensile tests were carried out on injection-molded pieces with a size of 75 × 5 × 4 mm^3 using a universal testing machine ELIB 50 from S.A.E. Ibertest (Madrid, Spain) equipped with a 5-kN load cell. The tests were performed as recommended by ISO 527-1:2012. The cross-head speed was set to 5 mm min^{-1}.

Shore D hardness was measured in a 676-D durometer from J. Bot Instruments (Barcelona, Spain) according to ISO 868:2003. Impact strength was also studied on

unnotched pieces with dimensions of 80 × 10 × 4 mm^3 in a 6-J Charpy pendulum from Metrotec S.A. (San Sebastián, Spain) following the guidelines of ISO 179-1:2010.

All samples were tested at room conditions, that is, 23 ºC and 50% RH, using at least six samples per formulation.

2.7. Thermomechanical characterization

Dynamic mechanical thermal analysis (DMTA) was performed using an AR-G2 oscillatory rheometer from TA Instruments (New Castle, DE, USA), which was equipped with a special clamp system for solid samples working in combined torsion-shear mode. The samples, with dimensions of 40 × 10 × 4 mm^3, were subjected to a temperature sweep from 30 ºC to 140 ºC at a constant heating rate of 2 ºC min^{-1}. The maximum deformation percentage (γ) was set to 0.1%. The storage modulus and the dynamic damping factor (tan δ) were obtained as a function of increasing temperature at a constant frequency of 1 Hz. DMTA tests were run in triplicate.

Dimensional stability was studied by measuring the coefficient of linear thermal expansion (CLTE) using a thermomechanical analyzer (TMA) Q400 model from TA Instruments. The test was performed on injection-molded pieces sizing 10 × 10 × 4 mm^3. The heating program was set from 0 ºC to 140 °C with a constant heating rate of 2 °C min^{-1} and a load of 0.02 N. CLTE measurements were performed in triplicate.

2.8. Disintegration tests

Disintegration in simulated composting conditions was conducted at 58 °C and 55% RH as indicated by ISO 20200. Injection-molded pieces sizing 10 × 10 × 4 mm^3 were placed in a carrier bag and buried in a controlled soil compost made of sawdust (40 wt.-%), rabbit-feed (30 wt.-%), ripe compost (10 wt.-%), corn starch (10 wt.-%), saccharose (5 wt.-%), corn seed oil (4 wt.-%), and urea (1 wt.-%). Samples were periodically

unburied from the composting facility, washed with distilled water, dried, and weighed in an analytical balance. The weight loss during disintegration was calculated using **Eq. 2**:

$$\text{Weight loss (\%)} = \left(\frac{W_0 - W_t}{W_0}\right) \cdot 100 \qquad \textbf{Equation 2}$$

Where W_0 is the initial dry weight of the sample and W_t is the weight of the sample after a bury time *t*. All tests were carried out in triplicate to ensure reliability.

3. Results and discussion

3.1. Morphology of orange peel flour

Figure 2 shows the size distribution of the OPF particles used for the preparation of the green composites. One can observe that the mean particle size was approximately 25 μm, being most of the particles smaller than 75 μm. The micro-sized structure of OPF is considered a positive aspect for their adhesion to the biopolymer matrix due to the total surface area of the fillers increases.[45, 46] The provided FESEM image of OPF, shown in the inset, also indicates that particles morphology was mostly heterogeneous. In addition, a rough perimeter was observed, which can be a consequence of the intensive crushing and milling processes applied to obtain the flour.

3.2. Thermal properties

Figure 3 shows the DSC thermograms of PLA and its green composite pieces with OPF obtained by injection molding. The main thermal parameters obtained by DSC are summarized in **Table 2**. The neat PLA pieces were characterized by having a glass transition temperature (T_g) and melting temperature (T_m) of approximately 64 °C and 171.5 °C, respectively, and a X_C value close to 24%. In addition, the biopolymer showed a cold crystallization process with a cold crystallization temperature (T_{CC}) of ~93 °C. The incorporation of AESO slightly increased the degree of crystallinity, that

is, the X_C value for the AESO-containing PLA piece was 28.5%. The value of T_g was reduced to ~60 °C while T_{CC} and T_m remained nearly constant.

The incorporation of OPF also reduced T_g to ~59 °C and induced a pronounced reduction in the crystallinity of the PLA pieces, that is, X_C was reduced to values of ~6%. This remarkable reduction of crystallinity can be produced due to transesterification between the particles and the PLA chains, leading to the formation of a more amorphous structure. However, it is worthy to note that the green composite pieces presented similar T_m values than the neat PLA piece, which indicates that the OPF presence did not alter the crystal type of the biopolymer or the lamellar thickness of its spherulites. In relation to T_{CC}, one can observe that there was a notable delay in the cold crystallization process. In particular, the green composite piece containing 10 wt.-% OPF without AESO showed a T_{CC} close to 108 °C, that is, 15 °C higher than the neat PLA piece. Therefore, it confirms that the OPF particles predominantly acted as anti-nucleating agent for PLA,[47] interrupting the folding or packing process of the PLA chains.

The green composite pieces containing AESO presented lower values of T_g, particularly in the 54–56 °C range. The incorporation of AESO also affected the process of cold crystallization of the pieces, which moved towards lower temperatures in relation to the green composite piece without AESO. The lowest value was observed for the AESO-containing green composite with 20 wt.-% OPF, showing a T_{CC} value around 99 °C. In this sense, one can consider that AESO acted as a plasticizer in the green composites. It typically increases free volume and reduces polymer–polymer interactions, allowing a greater mobility of the polymer chains and reducing both T_g and T_{CC} values.[48, 49] Nevertheless, this effect was relatively low in comparison to other plasticizers, such as poly(ethylene glycol) (PEG) and poly(propylene glycol) (PPG),[50, 51] acetyl tri-*n*-butyl

citrate (ATBC),[52] oligomeric lactic acid (OLA)[53], *etc.*, which have been reported to decrease T_g of PLA materials by 25–30 °C with contents in the 10–20 wt% range. In this sense, a reduction of T_g of only 2–3 °C has been recently observed in AESO-toughened PLA pieces.[40] The incorporation of higher percentages of lignocellulosic fillers, that is, 20–30 wt.-% OPF, into the PLA formulations containing 5 phr AESO produced a slight reduction in both T_{CC} and T_m while it resulted in an increase of the X_C values.

Figure 4 shows the TGA curves of the PLA and the green composite pieces. It can be observed that the incorporation of OPF significantly reduced the thermal stability of PLA. This also induced the development of two degradation stages, which are summarized in **Table 3**. The first one occurred in the temperature range of 200–350 °C, which corresponds to the decomposition of hemicelluloses at 200–300 °C and of celluloses at 300–350 °C.[54] This step overlapped with the PLA degradation and it became more significant as the percentage of OPF in the composite increased. The second stage took place from 400 to 500 ºC and it can be related to the degradation of the lignin fraction present in OPF.[55] The incorporation of OPF also resulted in a direct increase of the residual mass at 600 °C, producing values of ~3% for the green composite pieces with the highest filler content.

Interestingly, the addition of AESO slightly improved the thermal stability of PLA. In particular, the T_{deg} value of the neat PLA piece was around 362 °C and the addition of 5 phr AESO reduced it by 5 °C. A similar effect has been recently observed for PLA materials containing AESO[40] and epoxidized linseed oil (ELO)[56] and, hence, it potentially suggests that the molecular structure of the biopolymer was altered. This enhancement in the thermal stability suggests certain chemical interaction of AESO with both components of the green composite, by which the resultant linked

lignocellulosic fillers are expected to act as a physical barrier that obstructs the removal of volatile products produced during decomposition. This is an interesting result since one of the main drawbacks of most PLA plasticizers is related to the fact that they habitually lower the thermal stability of the biopolymer.[52, 57] This thermal degradation improvement was also observed for the green composite pieces containing AESO, though their resultant thermal stability was still slightly lower than that of the neat PLA.

3.3. Mechanical properties

Table 4 summarizes the effect of both OPF and AESO on the mechanical properties of the injection-molded PLA pieces. In relation to the tensile properties, one can observe that the PLA modulus increased with the addition of the multi-functionalized vegetable oil and, more significantly, of the lignocellulosic filler. While the neat PLA piece showed a Young modulus of ~1.97 GPa, it slightly increased to 2.12 and 2.71 GPa with the addition of 5 phr AESO and 10 wt.-% OPF, respectively. Furthermore, the modulus remained almost constant, that is, around 2.70–2.80 GPa, for green composite pieces containing AESO at all OPF loadings. For the lowest OPF content, that is, 10 wt.-%, the values of tensile strength also remained close to that of the neat PLA piece, that is, 66 MPa. However, higher filler contents reduced the tensile strength to values of approximately 50 and 40 MPa for the green composite pieces filled with 20 and 30 wt.-% OPF, respectively.

Since the elongation at break was also reduced in the green composite pieces, it can be considered that the lignocellulosic fillers acted as a stress concentrator. In particular, the elongation-at-break values decreased from 5.3%, for the neat PLA piece, to 4.5%, for the green composite piece containing 10 wt.-% OPF without AESO. This result points out the poor adhesion of the OPF particles to the biopolymer and probably their low dispersion in the PLA matrix. Therefore, the lignocellulosic fillers acted as a defect

rather than a reinforcement so that these cannot efficiently absorb the stresses or prevent the propagation of cracks.[58] However, the addition of 5 phr AESO led to a considerable increase in elongation at break up to 7.3%. This value represents an increment of approximately 40%, further indicating that the multi-functionalized vegetable oil provided some plasticization to the PLA matrix. Interestingly, AESO also improved the ductility of the green composite pieces. The carried out comparison of the injection-molded green composite piece at 10 wt.-% OPF with and without AESO shows that the addition of the multi-functionalized vegetable oil improved the elongation at break from 4.5% to 4.9%, that is, around 9%, while the tensile modulus and strength remained nearly constant. This improvement in the elongation at break allowed to achieve a green composite piece with a ductility relatively similar to that observed for the neat PLA piece.

Regarding hardness, the OPF addition also produced a moderate increase. In particular, the hardness value increased from 80.2, for the neat PLA piece, to 84.4, for the green composite piece containing 10 wt.-% OPF without AESO, which is the typical effect of a hard filler on a polymer matrix. While the addition to AESO did not provide any remarkable effect on the PLA hardness, the green composites containing AESO and with high contents OPF further increased the hardness of the injection-molded pieces. In particular, the highest D Shore hardness was observed for the PLA piece filled with 30 wt.-% OPF, that is, 85.2.

As opposite to hardness, the impact strength decreased after OPF incorporation. This was reduced from 22.8 kJ m^{-2}, for the neat PLA piece, to 18.1 kJ m^{-2}, for the green composite piece with 10 wt.-% OPF. Interestingly, the addition of AESO remarkably improved toughness of the PLA piece, increasing its impact strength up to 29.7 kJ m^{-2}, which means an improvement of approximately 30%. Similar results were also

observed, for instance, by Ferri *et al.*[59] for plasticized PLA with MLO, though it was also observed a saturation effect at a very low concentration. In the case of the AESO-containing green composite piece with 10 wt.-% OPF, a slight increase in the impact strength was also observed. This green composite piece presented an impact-strength value of 20.8 kJ m^{-2}, being very close to that of the neat PLA piece. However, for the green composite pieces with 20 and 30 wt.-% OPF, the decrease in impact strength was significant due to the relatively high filler content, which clearly compromises the pieces' capacity for energy absorption.

3.4. Thermomechanical properties

Figure 5 shows the dynamic behavior, obtained from DMTA in torsion mode, of the neat PLA and green composite pieces. In **Figure 5a**, which shows the evolution of the storage modulus *vs.* temperature, both the glass transition and cold crystallization processes can be observed. For the neat PLA piece, T_g was detected by a drop of the storage modulus of 2 orders in the 55–65 ºC range. Besides, the cold crystallization process occurred from 80 ºC, showing a slight increase in the storage modulus due to the formation of a stiffer material by a crystallinity increase. The OPF incorporation produced a remarkable increase of the storage modulus at temperatures below T_g and a slight delay in the temperature at which cold crystallization occurred, as it was stated above during the DSC analysis. For instance, at 40 ºC, the storage modulus increased from a value of 1.5 GPa, for the neat PLA piece, to a value of 2.1 GPa, in the case of the green composite piece with 10 wt.-% OPF. The addition of AESO also increased the storage modulus of PLA up to a value of 1.6 GPa at 40 ºC. In general, the curves for all green composite pieces shifted towards lower temperatures, thus indicating a slight decrease in T_g of PLA with an additional positive effect on the toughness.

In relation to the damping factor, in **Figure 5b** it can be observed that the peak of the neat PLA piece shifted to lower temperatures for the pieces containing both OPF and AESO. This decrease of the tan δ peak indicates a reduction of the alpha (α)-relaxation of the biopolymer, which is related to its T_g. Although this effect was noticeable for all the materials, it was more intense in the case of the green composites containing AESO in which it was reduced by ~5 °C. In addition, all green composite pieces presented higher values of tan δ than the neat PLA piece, which is a direct indication that the pieces presented a higher energy dissipation with improved toughness.[16]

In relation to the dimensional stability, as it can be observed in **Table 5**, all PLA pieces presented higher CLTE values above T_g than below T_g since the biopolymer chains were more readily available to move. Interestingly, AESO also provided certain interesting changes in the CLTE values. Specifically, below T_g, it decreased from 95.3 μm m^{-1} $ºC^{-1}$, for the neat PLA piece, to 91.7 μm m^{-1} $ºC^{-1}$, for the AESO-containing PLA piece. This effect has been previously ascribed to the formation of a long-chained or partially cross-linked structure due to the reaction of PLA with the multiple epoxy or acrylate groups present in AESO.[40] The addition of OPF further decreased the CLTE values below T_g, indicating that the pieces acquired more thermomechanical resistance. Above T_g, the CLTE value increased from 148.8 μm/m ºC, for the neat PLA piece, to 202.5 μm m^{-1} $ºC^{-1}$, for the PLA piece containing AESO. However, for the AESO-containing green composite pieces, a positive dimensional stabilization was observed. In particular, the green composites showed CLTE values in the 175–185 μm m^{-1} $ºC^{-1}$ range, therefore presenting an extraordinary thermomechanical response at high temperatures. One can also observe that the incorporation of OPF also reduced the T_g values of PLA, presenting values very similar to those above-reported by DSC. For

instance, for the green composite piece with the highest OPF content, that is, 30 wt.-%, the reduction was higher than 10 ºC in relation to the neat PLA piece.

3.5. Morphology of green composites

Figure 6 shows the fracture surface after the impact test of the injection-molded pieces of PLA and its green composites with OPF. The fracture of the neat PLA piece, shown in **Figure 6a**, shows the characteristic morphology of a brittle material with a low energy absorption. Both a micro-crack formation and a high roughness can be observed, showing no evidence of plastic deformation. In **Figure 6b**, as opposite, one can observe that the addition of AESO modified the surface fracture of the PLA piece. It changed from a rough surface to plastic-like morphology with the presence of some long filaments. This confirms the increase in toughness described above during the mechanical analysis. **Figure 6c** shows the fracture surface of the green composite containing 10 wt.-% OPF without AESO. This FESEM image revealed the presence of some voids, more likely produced from particle debonding during breaking, and also the large gaps in the interphase between the lignocellulosic particles and the biopolymer matrix. Therefore, the observed morphology fully confirmed the poor compatibility between both components of the green composite.

Interestingly, as shown in **Figure 6d** to **6f**, one can observe that the morphology of the fracture surfaces of all AESO-toughened green composites was remarkably different. Comparison of both FESEM images shown in **Figure 6d** and **6c**, that is, the fracture surfaces of the green composite at 10 wt.-% OPF with and without AESO, respectively, indicates that the presence of the multi-functionalized vegetable oil notably reduced the number of voids and also produced smaller gaps between the OPF particles and the PLA biopolymer. In addition, as it can be observed in **Figure 6f** for the green composite

piece with the highest OPF loading, that is, 30 wt.-%, the dispersion of the lignocellulosic fillers was relatively high.

3.6. Compatibilization of green composites

From the above-observed improvement in morphology, it can be established that the PLA–OPF adhesion increased in the injection-molded pieces after the AESO addition. Furthermore, AESO offered a more balanced mechanical and thermomechanical performance whilst the thermal properties were slightly improved. It has been considered that AESO induced certain plasticization on the PLA matrix, which increased ductility and toughness of the PLA and its green composites pieces. However, changes in T_g were relatively small, as determined by both DMTA and CLTE analysis. In the addition, the elongation at break, which is a direct measurement of the mechanical ductile properties, did not increase in a remarkable way as other plasticizers certainly do.[43] Therefore, in addition to a plasticizing effect, AESO induced certain interfacial adhesion between the OPF particles and the PLA matrix by which it promoted a moderate increase in elongation at break in combination to a significant improvement of the mechanical resistant properties. This improvement was further assessed based on the fact that the cold crystallization peak was delayed and the melting peak slightly shifted to lower temperatures while the crystallization degree was noticeably reduced.

Based on our previous research findings related to biopolymer composites and nanocomposites processed by REX with multi-functional low-M_W additives,[30, 41] it is proposed that AESO also acted as a reactive compatibilizer during melt processing, successfully establishing strong chemical ‘‘bridges” between the biopolymer chains and the lignocellulosic fillers. AESO, which is feasibly obtained from epoxidized soybean oil (ESO) by treatment with acrylic acid (AA),[40] is based on a chemical structure

containing multiple acrylate and epoxy groups. These functional groups are highly reactive, being then able to provide a chain-extension and/or cross-linking effect to polymers also containing functional groups. Indeed, AESO has been recently reported as an environmentally friendly additive for toughening PLA-based materials.[40, 43]

Therefore, **Figure 7** suggests the possible grafting mechanism of OPF onto the PLA macromolecular structure during melt processing. On the one hand, in the case of the biopolymer, ester bonds are proposed to be formed by the reaction of the terminal acid groups of the PLA chains with some of the multiple epoxy groups of AESO. In this sense, the mechanisms of epoxy ring-opening to produce chain extension in polyesters typically consists on glycidyl esterification of the carboxylic acid end groups, which precedes hydroxyl end group etherification.[60] In the case of polyesters, the reaction rate of the epoxy groups is known to be approximately 10–15 times higher with the carboxyl (–COOH) than with the hydroxyl group (–OH).[61] On the other hand, other epoxy groups present in AESO can simultaneously react with the –OH groups of the cellulose available on the surface of the OPF particles. This reaction generates C–O–C bonds with hydroxyl side group formation. Therefore, a new hybrid structure, namely a cellulose-grafted PLA composite, that is, cellulose-*g*-PLA composite, was formed.

3.7. Disintegration of green composites

Finally, disintegration tests in a controlled compost soil were carried out in order to ascertain the effect of both OPF and AESO on the PLA compostability. The weight loss of the injection-molded PLA-based pieces during disintegration in compost are plotted in **Figure 8**. In addition, **Figure 9** shows the visual aspect of the pieces evaluated during the disintegration test. One can observe that, after an incubation period of about two weeks, all pieces started an embrittlement process accompanied by the development of a dark-to-black color and a quick weight loss. It is also worthy to remark that the test was

conducted at 58 °C and 50% RH, that is, a relative high temperature and humidity, which are certainly favorable conditions for the hydrolytic degradation of PLA. Although it has been previously reported in the polymer literature that neat PLA disintegrates notably faster than its composites based on lignocellulosic fillers,[62, 63] the here-developed green composites presented similar degradation rates. In the case of the AESO-containing PLA piece and the green composite piece with 10 wt.-% OPF, the disintegration rate was even slightly faster than that the neat PLA piece during the first 4 weeks. In the case of the green composites containing AESO, these pieces showed a slightly slow degradation profile in the final weeks, particularly for the piece filled with 30 wt.-% OPF. After 8 weeks, the neat PLA piece lost over 98% of its initial weight while both the AESO-containing PLA piece and the green composite piece filled with 10 wt.-% OPF were fully degraded. For the AESO-containing green composites the weight loss reached values around 95%. Therefore, it can be concluded that neither the multi-functional vegetable oil or the lignocellulosic filler impair the compostability of the PLA pieces.

4. Conclusions

The present study describes the preparation and characterization of PLA/OPF composite pieces compatibilized with AESO, an environmentally friendly multi-functionalized additive that can be easily obtained from natural soybean oil. While the incorporation of OPF into PLA induced a remarkable reduction of both thermal stability and mechanical ductility, showing values of T_{deg} of 363 °C and values of elongation at break and impact strength of 4.5% and 18.1 kJ m^{-2}, respectively, the addition of only 5 phr AESO successfully enhanced the thermal, mechanical, and thermomechanical properties of the green composites. In particular, for the AESO-compatibilized green composite piece filled with 10 wt.-%, the elongation at break and impact strength were approximately

9% and 13% higher, respectively. However, in the case of the green composite pieces with higher fillers contents, that is, 20 and 30 wt.-% OPF, a significant decrease in ductility was observed. The compatibilization achieved was ascribed to a dual effect of plasticization in combination with melt grafting of the OPF particles onto the PLA chains provided by the multiple functional groups present in the chemical structure of AESO.

The here-obtained results indicate that OPF, a large by-product of the food juice industry, can be successfully incorporated up to 10 wt.-% into PLA by melt processing in the presence of AESO without compromising the physical properties and compostability of the biopolymer. It can be concluded that AESO, similar to other multi-functionalized vegetable oils, can be used as a reactive additive to enhance the compatibility between biopolymers and lignocellulosic fillers in green composite articles and, thus, it can potentially contribute to the development of sustainable polymer technologies.

5. Acknowledgements

This research was supported by the Spanish Ministry of Economy and Competitiveness (MINECO) program numbers MAT2014-59242-C2-1-R and AGL2015-63855-C2-1-R. L. Quiles-Carrillo also wants to thank the Spanish Ministry of Education, Culture, and Sports (MECD) for the financial support through a FPU grant number FPU15/03812.

References

1 L. Quiles-Carrillo, N. Montanes, T. Boronat, R. Balart and S. Torres-Giner, *Polymer Testing* **61:**421-429 (2017).

2 E. Chiellini, P. Cinelli, F. Chiellini and S. H. Imam, *Macromolecular bioscience* **4:**218-231 (2004).

3 S. K. Majhi, S. K. Nayak, S. Mohanty and L. Unnikrishnan, *International Journal of Plastics Technology* **14:**57-75 (2010).

4 V. K. Thakur, M. K. Thakur, P. Raghavan and M. R. Kessler, *ACS Sustainable Chemistry & Engineering* **2:**1072-1092 (2014).

5 H.-S. Yang, H.-J. Kim, J. Son, H.-J. Park, B.-J. Lee and T.-S. Hwang, *Composite Structures* **63:**305-312 (2004).

6 S. Cheng, K.-t. Lau, T. Liu, Y. Zhao, P.-M. Lam and Y. Yin, *Composites Part B: Engineering* **40:**650-654 (2009).

7 M. Huda, A. Mohanty, L. Drzal, E. Schut and M. Misra, *Journal of Materials Science* **40:**4221-4229 (2005).

8 K. M. Nampoothiri, N. R. Nair and R. P. John, *Bioresource technology* **101:**8493-8501 (2010).

9 G. Koronis, A. Silva and M. Fontul, *Composites Part B: Engineering* **44:**120-127 (2013).

10 M. P. Dicker, P. F. Duckworth, A. B. Baker, G. Francois, M. K. Hazzard and P. M. Weaver, *Composites part A: applied science and manufacturing* **56:**280-289 (2014).

11 P. K. Bajpai, I. Singh and J. Madaan, *Journal of Thermoplastic Composite Materials* **27:**52-81 (2014).

12 E. Zini and M. Scandola, *Polymer composites* **32:**1905-1915 (2011).

13 Y.-F. Shih and C.-C. Huang, *Journal of polymer Research* **18:**2335-2340 (2011).

14 M. Laka, S. Chernyavskaya and M. Maskavs, *Mechanics of composite materials* **39:**183-188 (2003).

15 H. A. Khalil, A. Bhat and A. I. Yusra, *Carbohydrate Polymers* **87:**963-979 (2012).

16 S. Torres-Giner, N. Montanes, O. Fenollar, D. García-Sanoguera and R. Balart, *Materials & Design* **108:**648-658 (2016).

17 B. Rai, G. Kumar, V. Tyagi, R. Diwan and U. Niyogi, *Journal of Polymer Materials* **32:**305 (2015).

18 S. Karlssion and B. S. Ndazi(2011).

19 A. Yussuf, I. Massoumi and A. Hassan, *Journal of Polymers and the Environment* **18:**422-429 (2010).

20 Y. Nishikawa, N. Nagase and K. Fukushima, *Journal of Environment and Engineering* **4:**124-134 (2009).

21 D. Garcia□Garcia, A. Carbonell□Verdu, A. Jordá□Vilaplana, R. Balart and D. Garcia□Sanoguera, *Journal of Applied Polymer Science* **133:**(2016).

22 S. Sanchez-Vazquez, H. Hailes and J. Evans, *Polymer Reviews* **53:**627-694 (2013).

23 S. Torres-Giner, N. Montanes, V. Fombuena, T. Boronat and L. Sanchez-Nacher, *Advances in Polymer Technology* DOI: 10.1002/adv.21789 (2016).

24 B. Ferrero, V. Fombuena, O. Fenollar, T. Boronat and R. Balart, *Polymer Composites* **36:**1378-1385 (2015).

25 L. Coltro, A. L. Mourad, R. M. Kletecke, T. A. Mendonça and S. P. Germer, *The International Journal of Life Cycle Assessment* **14:**656-664 (2009).
26 K. Rezzadori, S. Benedetti and E. Amante, *Food and bioproducts processing* **90:**606-614 (2012).
27 J. S. Borah and D. S. Kim, *Korean Journal of Chemical Engineering* **33:**3035-3049 (2016).
28 H.-S. Yang, H.-J. Kim, H.-J. Park, B.-J. Lee and T.-S. Hwang, *Composite Structures* **72:**429-437 (2006).
29 J.-M. Raquez, P. Degée, Y. Nabar, R. Narayan and P. Dubois, *Comptes Rendus Chimie* **9:**1370-1379 (2006).
30 S. Torres-Giner, N. Montanes, T. Boronat, L. Quiles-Carrillo and R. Balart, *European Polymer Journal* **84:**693-707 (2016).
31 Q.-K. Meng, M.-C. Heuzey and P. Carreau, *International Polymer Processing* **27:**505-516 (2012).
32 N. Najafi, M. Heuzey and P. Carreau, *Composites Science and Technology* **72:**608-615 (2012).
33 J.-F. Zhang and X. Sun, *Biomacromolecules* **5:**1446-1451 (2004).
34 V. H. Orozco, W. Brostow, W. Chonkaew and B. L. Lopez, Preparation and characterization of poly (Lactic acid)□g□maleic anhydride+ starch blends, in *Macromolecular symposia*. Wiley Online Library, pp. 69-80 (2009).
35 Z. Xiong, L. Zhang, S. Ma, Y. Yang, C. Zhang, Z. Tang and J. Zhu, *Carbohydrate polymers* **94:**235-243 (2013).
36 A. A. Mamun, H.-P. Heim, D. H. Beg, T. S. Kim and S. H. Ahmad, *Composites Part A: Applied Science and Manufacturing* **53:**160-167 (2013).
37 D. García-García, A. Carbonell, M. Samper, D. García-Sanoguera and R. Balart, *Composites Part B: Engineering* **78:**256-265 (2015).
38 D. Garcia□Garcia, O. Fenollar, V. Fombuena, J. Lopez□Martinez and R. Balart, *Macromolecular Materials and Engineering* (2016).
39 L. Quiles-Carrillo, M. M. Blanes-Martínez, N. Montanes, O. Fenollar, S. Torres-Giner and R. Balart, *European Polymer Journal* **98:**402-410 (2018).
40 L. Quiles-Carrillo, S. Duart, N. Montanes, S. Torres-Giner and R. Balart, *Materials and Design* **140:**54-63 (2018).
41 L. Quiles-Carrillo, N. Montanes, C. Sammon, R. Balart and S. Torres-Giner, *Industrial Crops and Products* **111:**878-888 (2018).
42 Z. Xiong, Y. Yang, J. Feng, X. Zhang, C. Zhang, Z. Tang and J. Zhu, *Carbohydrate polymers* **92:**810-816 (2013).
43 S. C. Mauck, S. Wang, W. Ding, B. J. Rohde, C. K. Fortune, G. Yang, S.-K. Ahn and M. L. Robertson, *Macromolecules* **49:**1605-1615 (2016).
44 S. Torres-Giner, J. V. Gimeno-Alcañiz, M. J. Ocio and J. M. Lagaron, *Journal of Applied Polymer Science* **122:**914-925 (2011).
45 J. E. Crespo, R. Balart, L. Sanchez and J. Lopez, *International Journal of Adhesion and Adhesives* **27:**422-428 (2007).
46 J. E. Crespo, L. Sanchez, F. Parres and J. López, *Polymer Composites* **28:**71-77 (2007).
47 S. K. Hosseinihashemi, A. Eshghi, N. Ayrilmis and H. Khademieslam, *BioResources* **11:**6768-6779 (2016).
48 M. P. Arrieta, M. D. Samper, J. López and A. Jiménez, *Journal of Polymers and the Environment* **22:**460 (2014).
49 B. W. Chieng, N. A. Ibrahim, Y. Y. Then and Y. Y. Loo, *Molecules* **19:**16024-16038 (2014).

50 Z. Kulinski, E. Piorkowska, K. Gadzinowska and M. Stasiak, *Biomacromolecules* **7:**2128-2135 (2006).
51 M. Kowalczyk, M. Pluta, E. Piorkowska and N. Krasnikova, *Journal of Applied Polymer Science* **125:**4292-4301 (2012).
52 M. P. Arrieta, M. d. M. Castro-López, E. Rayón, L. F. Barral-Losada, J. M. López-Vilariño, J. López and M. V. González-Rodríguez, *Journal of Agricultural and Food Chemistry* **62:**10170-10180 (2014).
53 N. Burgos, V. P. Martino and A. Jiménez, *Polymer Degradation and Stability* **98:**651-658 (2013).
54 K. S. Chun, S. Husseinsyah and H. Osman, *Journal of Polymer Research* **19:**1-8 (2012).
55 S.-H. Lee and S. Wang, *Composites Part A: Applied Science and Manufacturing* **37:**80-91 (2006).
56 J. Balart, V. Fombuena, O. Fenollar, T. Boronat and L. Sánchez-Nacher, *Composites Part B: Engineering* **86:**168-177 (2016).
57 K.-M. Choi, S.-W. Lim, M.-C. Choi, Y.-M. Kim, D.-H. Han and C.-S. Ha, *Polymer Bulletin* **71:**3305-3321 (2014).
58 P. S. Delgado, S. L. B. Lana, E. Ayres, P. O. S. Patrício and R. L. Oréfice, *Materials Research* **15:**639-644 (2012).
59 J. M. Ferri, D. Garcia□Garcia, N. Montanes, O. Fenollar and R. Balart, *Polymer International* **66:**882-891 (2017).
60 M. Villalobos, A. Awojulu, T. Greeley, G. Turco and G. Deeter, *Energy* **31:**3227-3234 (2006).
61 R. Al-Itry, K. Lamnawar and A. Maazouz, *Polymer Degradation and Stability* **97:**1898-1914 (2012).
62 R. Kumar, M. Yakubu and R. Anandjiwala(2010).
63 A. P. Mathew, K. Oksman and M. Sain, *Journal of applied polymer science* **97:**2014-2025 (2005).

Table 1. Summary of the prepared compositions according to the weight content (wt.-%) of polylactide (PLA) and orange peel flour (OPF) in which acrylated epoxidized soybean oil (AESO) was added as parts per hundred resin (phr) of PLA/OPF composite.

Sample	**PLA (wt.-%)**	**OPF (wt.-%)**	**AESO (phr)**
PLA	100	0	0
PLA + AESO	100	0	5
PLA + 10 wt.-% OPF	90	10	0
PLA + AESO + 10 wt.-% OPF	90	10	5
PLA + AESO + 20 wt.-% OPF	80	20	5
PLA + AESO + 30 wt.-% OPF	70	30	5

Table 2. Summary of the main thermal parameters obtained by differential scanning calorimetry (DSC) in terms of glass transition temperature (T_g), normalized enthalpy of crystallization (ΔH_{CC}), cold crystallization temperature (T_{CC}), normalized enthalpy of melting (ΔH_m), melting temperature (T_m), and degree of crystallinity (X_C) of the injection-molded green composite pieces based on polylactide (PLA), orange peel flour (OPF), and acrylated epoxidized soybean oil (AESO).

Sample	**T_g (ºC)**	**ΔH_{CC} (J/g)**	**T_{CC} (ºC)**	**ΔH_m (J/g)**	**T_m (ºC)**	**X_C (%)**
PLA	63.9 ± 0.5	16.69 ± 0.26	92.7 ± 0.4	38.86 ± 0.31	171.5 ± 0.4	23.84 ± 0.86
PLA + AESO	59.9 ± 0.7	17.04 ± 0.49	92.9 ± 0.9	42.28 ± 0.63	171.9 ± 0.5	28.50 ± 0.94
PLA + 10 wt.-% OPF	59.1 ± 1.9	26.93 ± 0.41	107.8 ± 0.8	31.97 ± 0.52	172.4 ± 0.8	6.02 ± 0.84
PLA + AESO + 10 wt.-% OPF	55.9 ± 1.5	28.08 ± 0.28	103.1 ± 0.4	34.70 ± 0.39	170.6 ± 0.7	8.31 ± 0.35
PLA + AESO + 20 wt.-% OPF	54.4 ± 0.8	19.94 ± 0.35	98.9 ± 0.2	32.43 ± 0.46	170.0 ± 0.3	17.62 ± 0.33
PLA + AESO + 30 wt.-% OPF	54.1 ± 0.6	19.02 ± 0.31	101.5 ± 0.4	28.18 ± 0.41	169.6 ± 0.6	14.77 ± 0.44

Table 3. Thermal degradation steps and degradation temperature (T_{deg}) obtained by thermogravimetric analysis (TGA) of the injection-molded green composite pieces based on polylactide (PLA), orange peel flour (OPF), and acrylated epoxidized soybean oil (AESO).

Sample	1st step			2nd step			T_{deg} (°C)
	Onset (°C)	Endset (°C)	Mass loss (%)	Onset (°C)	Endset (°C)	Mass loss (%)	
PLA	329.8 ± 1.0	386.3 ± 0.9	99.5 ± 0.1	-	-	-	361.8 ± 1.5
PLA + AESO	339.9 ± 1.0	396.2 ± 1.1	98.8 ± 0.2	-	-	-	366.8 ± 1.2
PLA + 10 wt.-% OPF	335.6 ± 1.6	384.1 ± 0.8	92.5 ± 0.9	384.1 ± 0.9	488.8 ± 1.1	98.3 ± 0.1	362.6 ± 1.8
PLA + AESO + 10 wt.-% OPF	329.5 ± 1.0	381.3 ± 1.1	89.5 ± 0.6	381.3 ± 1.1	483.9 ± 1.0	98.3 ± 0.1	358.5 ± 1.4
PLA + AESO + 20 wt.-% OPF	328.4 ± 1.2	380.5 ± 0.9	85.2 ± 0.9	380.5 ± 1.2	507.9 ± 1.1	96.9 ± 0.1	359.3 ± 1.1
PLA + AESO + 30 wt.-% OPF	326.2 ± 1.1	373.9 ± 0.8	80.1 ± 0.8	376.9 ± 1.1	541.4 ± 0.9	96.9 ± 0.1	357.6 ± 1.4

Table 4. Mechanical properties in terms of tensile modulus (E), tensile strength at yield (σ_y), elongation at break (ε_b), D shore hardness, and impact strength of the injection-molded green composite pieces based on polylactide (PLA), orange peel flour (OPF), and acrylated epoxidized soybean oil (AESO).

Sample	**E (MPa)**	**σ_y (MPa)**	**ε_b (%)**	**D Shore hardness**	**Impact strength (kJ/m^2)**
PLA	1972.4 ± 95.4	65.9 ± 1.8	5.3 ± 1.0	80.2 ± 1.1	22.8 ± 1.1
PLA + AESO	2118.9 ± 65.9	64.6 ± 0.7	7.3 ± 0.4	81.4 ± 0.6	29.7 ± 0.8
PLA + 10 wt.-% OPF	2713.9 ± 103.5	64.3 ± 0.9	4.5 ± 0.3	84.4 ± 1.1	18.1 ± 0.7
PLA + AESO + 10 wt.-% OPF	2679.2 ± 81.4	63.4 ± 1.1	4.9 ± 0.2	84.6 ± 0.5	20.8 ± 0.5
PLA + AESO + 20 wt.-% OPF	2670.9 ± 115.0	50.3 ± 2.1	4.5 ± 0.4	84.7 ± 1.1	14.6 ± 0.8
PLA + AESO + 30 wt.-% OPF	2750.4 ± 103.6	40.1 ± 0.9	4.0 ± 0.4	85.2 ± 1.8	11.9 ± 0.7

Table 5. Coefficients of linear thermal expansion (CLTE) and glass transition temperature (T_g) of the injection-molded green composite pieces based on polylactide (PLA), orange peel flour (OPF), and acrylated epoxidized soybean oil (AESO).

Sample	**CLTE below T_g (µm/m°C)**	**CLTE above T_g (µm/m°C)**	**T_g (°C)**
PLA	95.3 ± 3.5	148.8 ± 2.3	65.7 ± 1.3
PLA + AESO	91.7 ± 2.2	202.5 ± 3.8	62.6 ± 2.2
PLA + 10 wt.-% OPF	83.8 ± 2.9	172.7 ± 1.9	60.8 ± 1.9
PLA + AESO + 10 wt.-% OPF	88.4 ± 3.1	173.8 ± 2.8	58.6 ± 1.5
PLA + AESO + 20 wt.-% OPF	88.2 ± 4.2	175.6 ± 2.6	56.9 ± 1.8
PLA + AESO + 30 wt.-% OPF	86.6 ± 2.6	184.5 ± 4.0	56.1 ± 1.9

Figure captions

Figure 1. a) As-received fresh oranges, b) Dried orange peel; c) Crushed orange peel particles; d) Orange peel flour (OPF) obtained after milling.

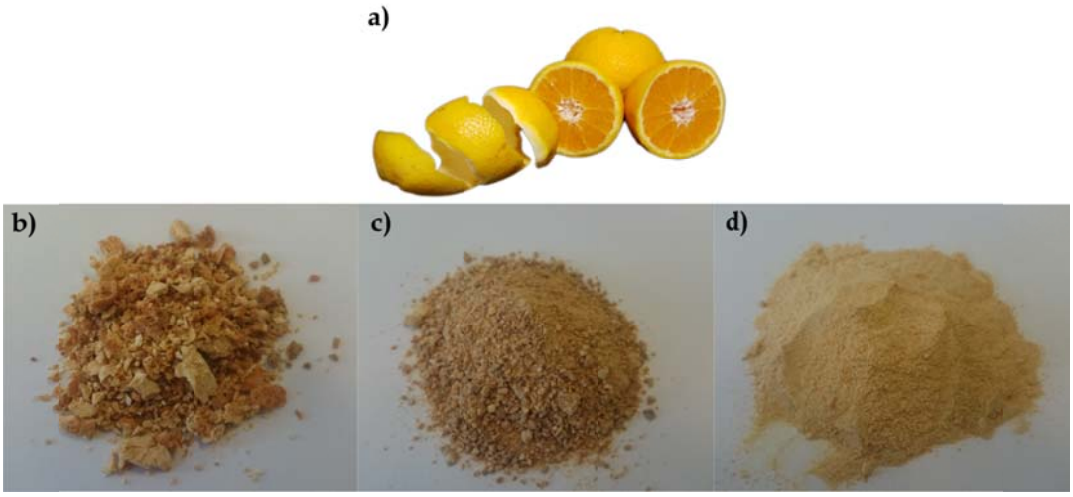

Figure 2. Histogram of orange peel flour (OPF) particles with field emission scanning electron microscope (FESEM) image of OPF. Image was taken with a magnification of 500× and scale marker is 10 μm.

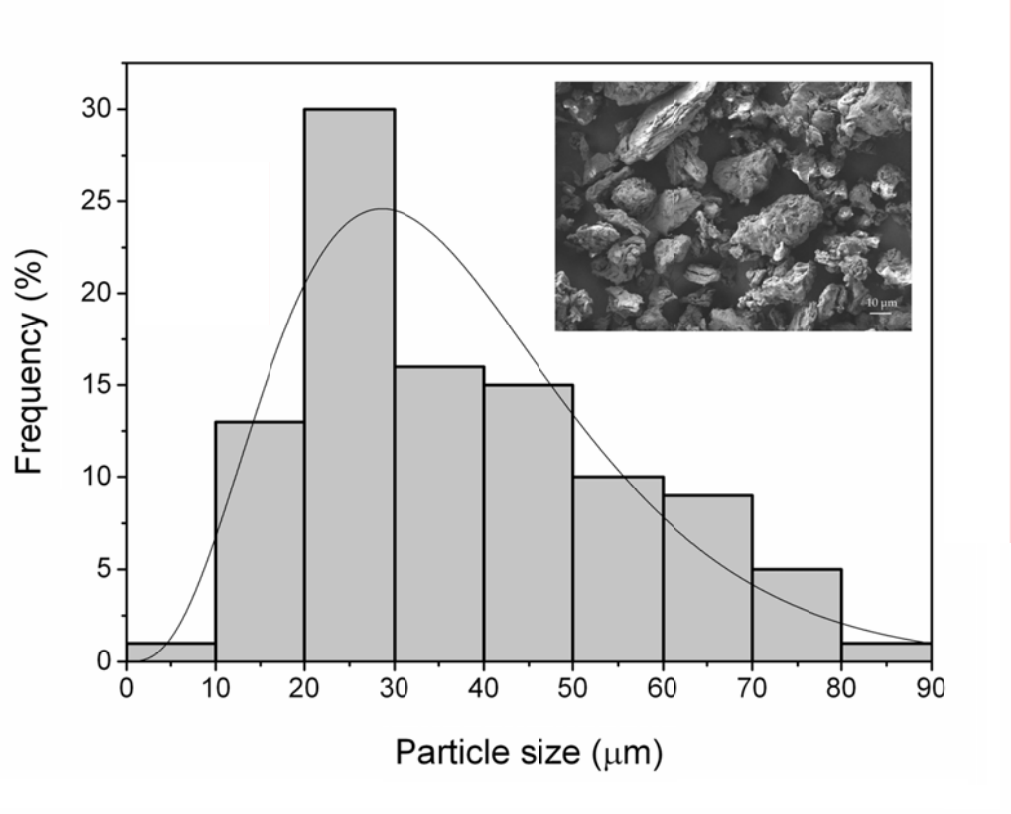

Figure 3. Differential scanning calorimetry (DSC) thermograms of the injection-molded green composite pieces based on polylactide (PLA), orange peel flour (OPF), and acrylated epoxidized soybean oil (AESO).

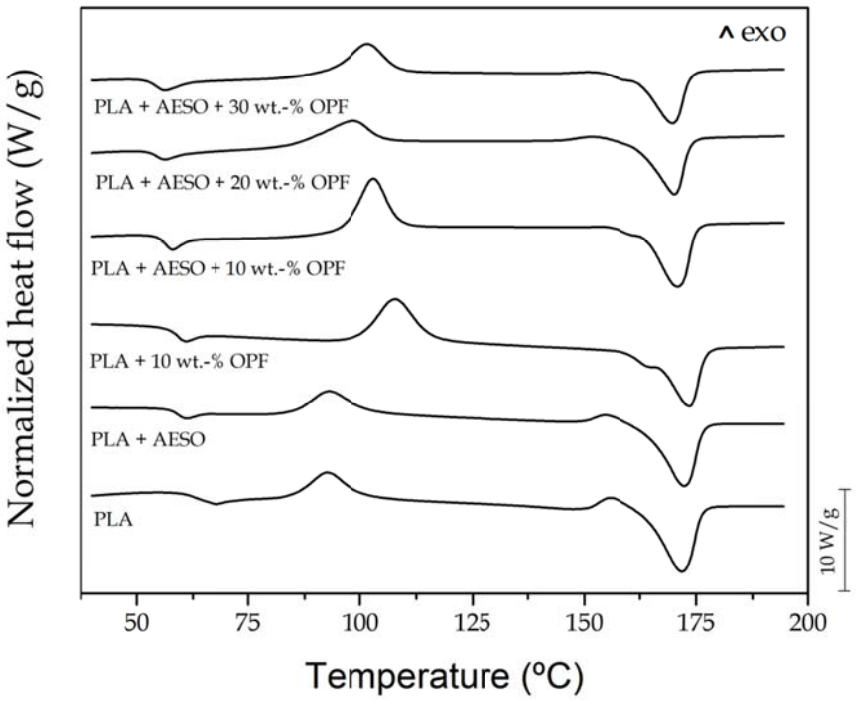

Figure 4. Thermogravimetric analysis (TGA) curves of the injection-molded green composite pieces based on polylactide (PLA), orange peel flour (OPF), and acrylated epoxidized soybean oil (AESO): a) Mass loss *vs.* temperature; b) First derivative *vs.* temperature.

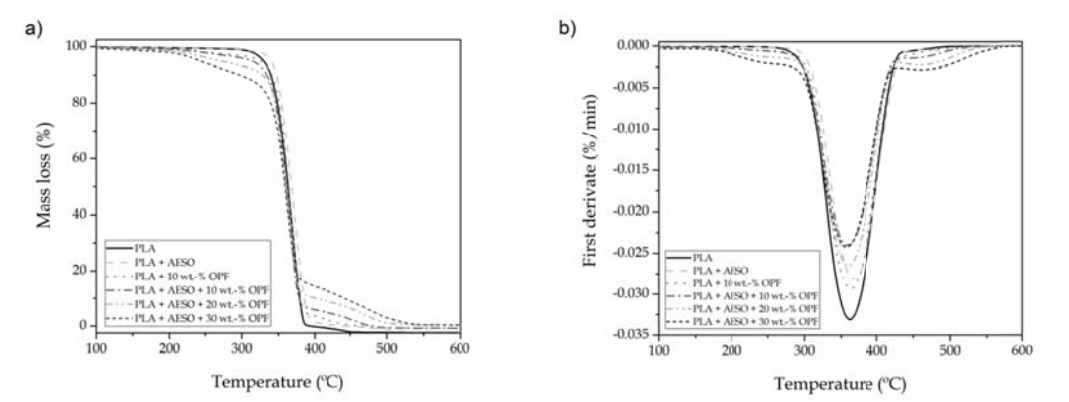

Figure 5. Dynamic mechanical thermal analysis (DMTA) curves of the injection-molded green composite pieces based on polylactide (PLA), orange peel flour (OPF), and acrylated epoxidized soybean oil (AESO): a) Storage modulus; b) Damping factor (tan δ).

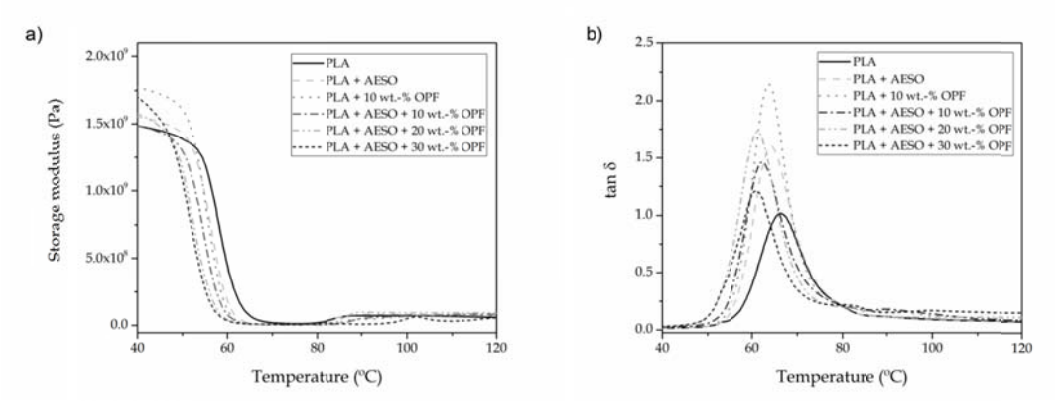

Figure 6. Field emission scanning electron microscopy (FESEM) images of fracture surface of the injection-molded pieces of: a) polylactide (PLA); b) PLA containing acrylated epoxidized soybean oil (AESO); c) PLA filled with 10 wt.-% orange peel flour (OPF); d) PLA + AESO + 10 wt.-% OPF; e) PLA + AESO + 20 wt.-% OPF; f) PLA + AESO + 30 wt.-% OPF.

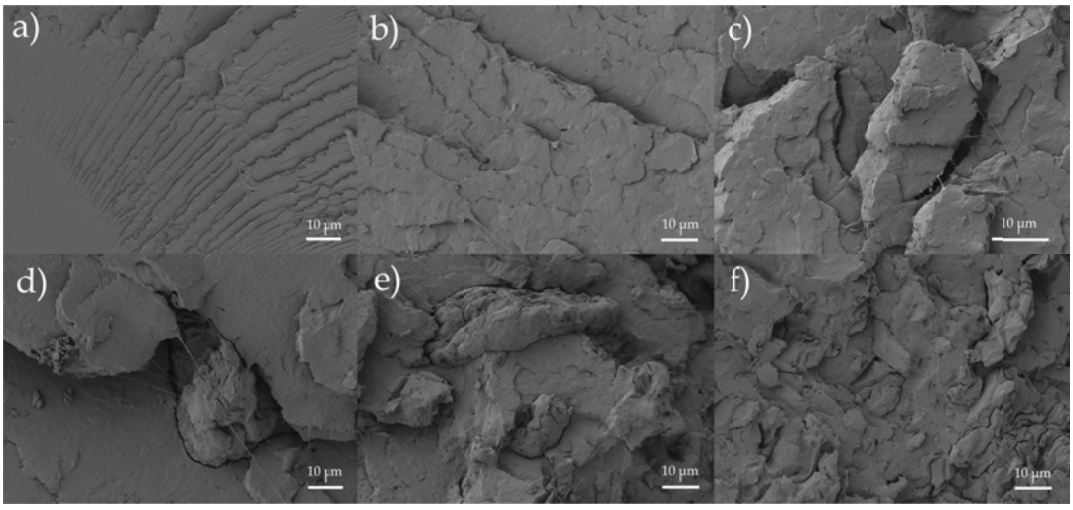

Figure 7. Schematic representation of the melt grafting of orange peel flour (OPF) onto polylactide (PLA) by acrylated epoxidized soybean oil (AESO).

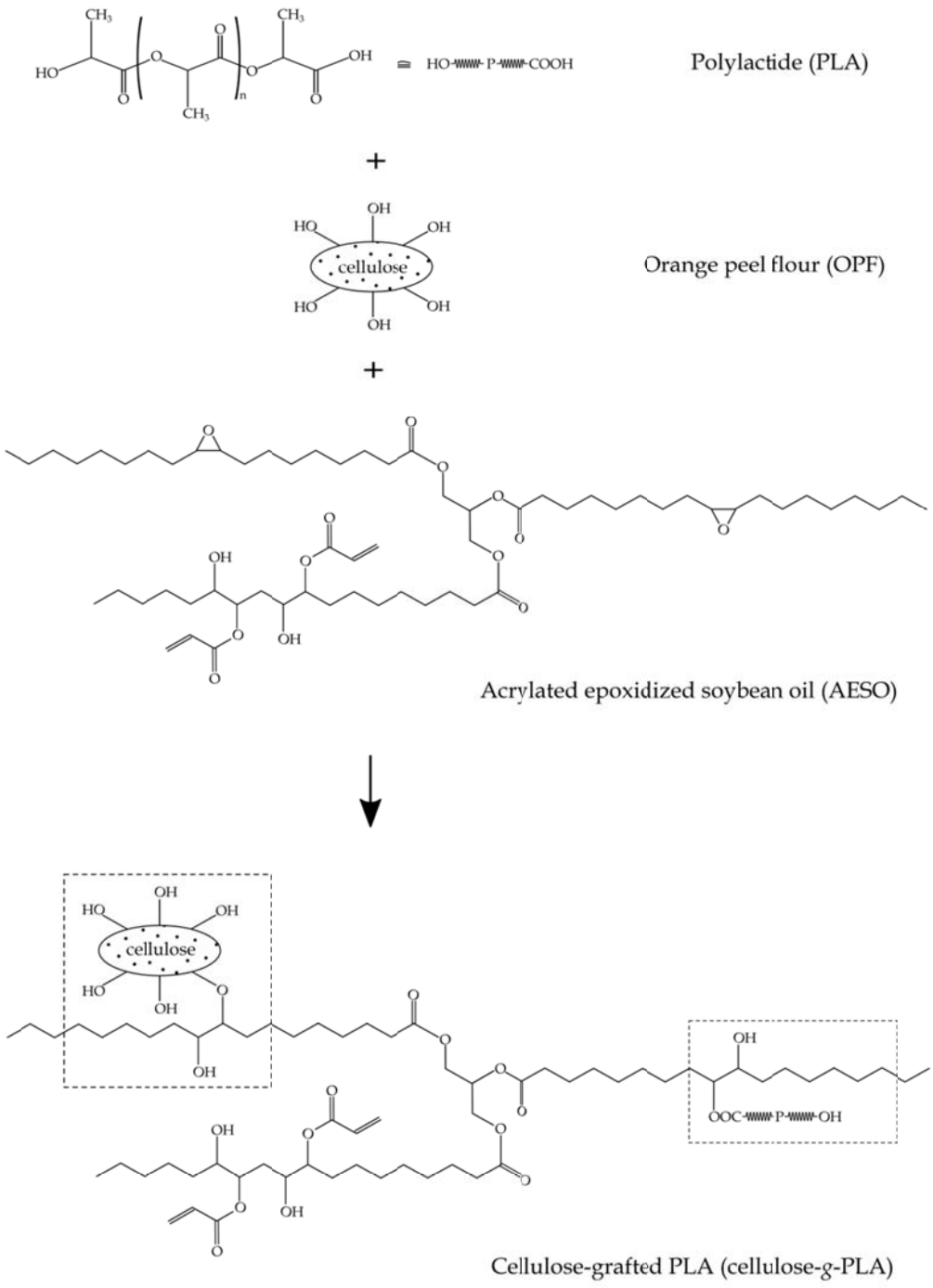

Figure 8. Percentage of weight loss as a function of the elapsed time during the disintegration test in controlled compost soil of the injection-molded green composite pieces based on polylactide (PLA), orange peel flour (OPF), and acrylated epoxidized soybean oil (AESO).

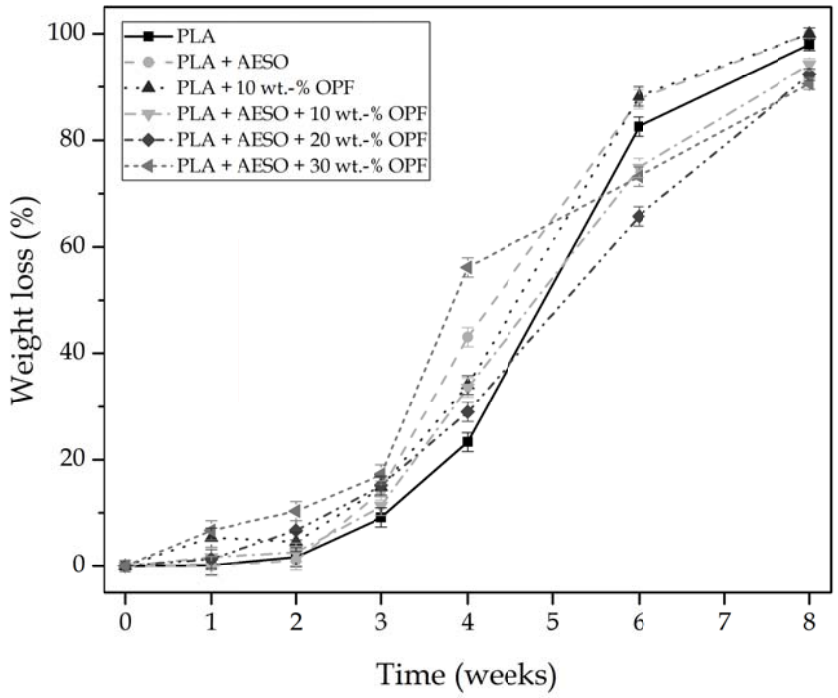

Figure 9. Visual aspect during the disintegration test in controlled compost soil of the injection-molded pieces of: a) polylactide (PLA); b) PLA containing acrylated epoxidized soybean oil (AESO); c) PLA filled with 10 wt.-% orange peel flour (OPF); d) PLA + AESO + 10 wt.-% OPF; e) PLA + AESO + 20 wt.-% OPF; f) PLA + AESO + 30 wt.-% OPF.

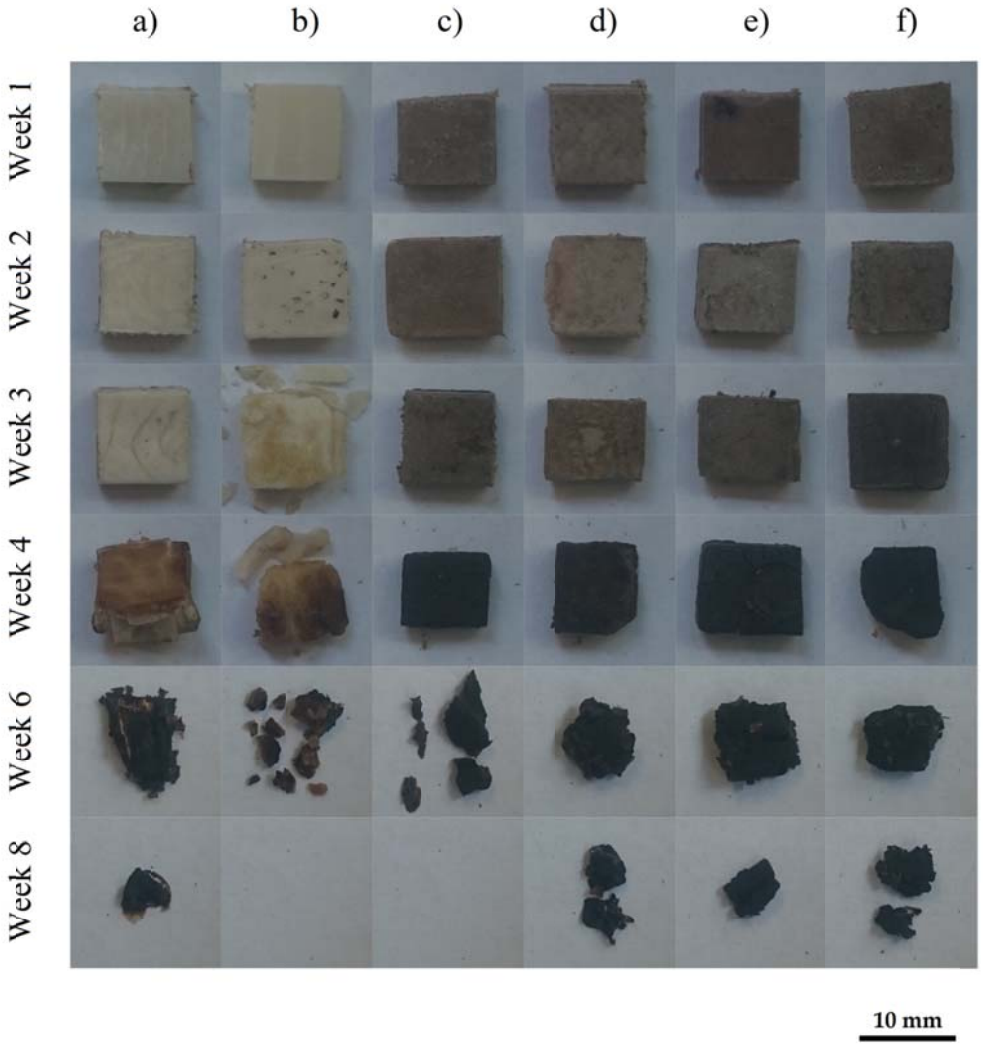
a)
b)
c)
d)
e)
f)
Week 1
Week 2
Week 3
Week 4
Week 6
Week 8
10 mm